Journal of Computational Science & Engineering 1 (2011) 33-41

Journal of Computational Science & Engineering

Available at http://icse.qdu.edu.cn ISSN 1710-4068

Cationic S-doped anatase TiO_2: a DFT study

Fenghui Tian[1*], Chengbu Liu[2], Wenwen Zhao[1], Xiaobin Wang[1], Zonghua Wang[1] and Jimmy C.Yu[3]

[1] *Institute of Computational Science and Engineering, Department of Chemistry, and Department of Physics, Qingdao University, Qingdao, 266071, China*

[2] *Institute of Theoretical Chemistry, Shandong University, Jinan, 250100 China*

[3] *Department of Chemistry, Environmental Science Programme and Centre of Novel Functional Molecules, The Chinese University of Hong Kong, Shatin, New Territories, Hong Kong, China*

Article Information

Article history:
Received 10 January 2011
Revised 13 January 2011
Accepted 23 January 2011
Available online 25 January 2011

Keywords:
TiO_2
Cationic S doping
Visible light photocatalysis
DFT

Abstract

Band gap engineering by doping is a good method to get a visible-light-driven photoca-talyst. Density functional theory (DFT) calculations are used to characterize the doping effect of S substituting for Ti in anatase TiO_2. Electronic structure analysis indicated that, just as in the anionic doping case (TiO_2-xSx: S substitute for O), the presence of an impurity state in the band gap near valence band O2p induced the visible light activity. Excitations from the impurity state to conduction band may be responsible for the red shift of absorption edge observed in the cationic S-doped TiO_2. Doping concentration dependent behavior of band gap energy and red shift of absorption edge for Ti1-xSxO_2 is also evidenced just as that for TiO_2-xSx. Differences exist in the composition and relative position of the impurity state. Partial density of states analysis shows that it is a mixing of S3p, S3s and Ti3d. Comparing with anionic S, N-doped TiO_2, the stronger absorption for Ti1-xSxO_2 is evidenced in our calculation. This may be a sign of its observed good performance in photocatalysis.

1. Introduction

Titanium dioxide (TiO_2) is a well-known photocatalyst because of its cheap, nontoxic peculiarities and stable, efficient perform-ances in the depuration of air and water. However, it is activated only under UV light irradiation (about 3% of the solar spectrum) because of its large band gap (3.2eV for anatase). So, it is in urgent need to develop efficient visible-light-driven photocatalysts by modification of TiO_2 which allow the main part of the solar spectrum (45% or so) to be used. Doping with transition metals is one of the methods to tailor the band gap of TiO_2, but this kind

* Corresponding author. E-mail: *tfh@qdu.edu.cn*

of doped TiO_2 generally has lower photocatalytic activity because of thermal instability and higher carrier recombination rate [1]. Recently, nonmetal- doped TiO_2 received a lot of attention as the doping of the nonmetals (S, N, C, B, P, F, etc.) could efficiently extend the photore- sponse of TiO_2 to low energy (visible) region [2-27].

Commonly, as a two-element crystal, TiO_2 could provide three kinds of positions for the impurity to occupy on, the O site, the Ti site and the interstitial site. And the doping impurity usually displays as an anion on the O site and a cation on the Ti site. Since the distinct visible light activity of the anionic N-doped TiO_2 with N substituting for O was disclosed [2], a large number of efforts were evoked on the anionic doping of non-metal elements in order to transform anatase TiO_2 to be visible light active. Among them, quite a lot of successful reports on different non-metal elements anionic doping, e.g. $TiO_{2-x}N_x$ [2-8], $TiO_{2-x}C_x$ [9], $TiO_{2-x}B_x$ [10], $TiO_{2-x}F_x$ [12], and $TiO_{2-x}S_x$ [13-15] etc., seemed to validate that the most suitable position for the non-metal element is the O site. It is accepted that non-metals usually dope as an anion to alternate the electronic structure and optical absorption property of TiO_2, and ultimately, to induce the visible light activity for it.

In this context, a report on S substitute for Ti as a cation in anatase TiO_2 aroused us much attention. It is reported that the photoabsorption of $Ti_{1-x}S_xO_2$ in the visible region is stronger than that of anionic S, N-doped TiO_2 and its photocatalytic activity is higher than the anionic S- and N-doped one by Ohno et al. [16-17]. Moreover, efficient visible-light-induced photocatalytic disinfection on cationic S-doped nanocrys- talline TiO_2 was also reported by Yu et al. [18]. In fact, substitutional doping had been applied to the modification of TiO_2 so as to obtain visible light active photocatalyst for a long time. The initial efforts were concentrated on transition metals substitut- ing for Ti as cations [1]. Only due to the gradually emerging defects mentioned above, a demand for a new kind of candidate was stimulated. According to the literatures, dislike the d orbital of transitional metals to provide doping level in the middle of band gap so that acting as a centre of electron-hole recombination [19], anionic doping of non-metals has a better performance in these sides. For example, N2p and S3p usually reside close to the upper edge of valence band O2p in anionic doping [2-3, 5-8, 13-15]. This also explains why so many investigations concentrated on the non-metal anionic doping of TiO_2. When S substitutes on Ti site, it will incorporate into TiO_2 lattice as a cation according to experiment results [16-18]. Our efforts on the anionic S-doped anatase TiO_2 helped us realize that S3p is a very suitable orbital to interact with O2p when S is doping as an anion [15]. What will the S do on the Ti sites? Our density functional calculation will try to disclose it.

Calculation results show that cationic S-doped TiO_2 indeed have a better visible light absorption than anionic S, N-doped TiO_2. The reason we speculated is related to the position of the impurity state in the band gap. The visible light activity of the doped material is due to the presence of the impurity state in the band gap slightly above the upper edge of valence band, similar to that of anionic S doping. In addition, the concentration-dependent behavior of band gap energy and absorption property of cationic S-doped TiO_2 is also concerned.

2. Computational details

The plane-wave-based density functional theory (DFT) calculation was performed using the CASTEP program [28] with the core orbitals replaced by ultrasoft pseudo-potentials, and a kinetic energy cutoff of 480eV. We choose to consider 108, 72 and 24 atom supercells denoted as (b), (c) and (d), with doping concentration of 0.0093, 0.0139 and 0.0417, respectively. The doping effects were modeled by replacing one Ti atom with one doping atom. Pure TiO_2 named (a) was calculated as a comparison. To minish error, we try to keep the doping atom close to the centre of the supercell. All the electronic structures and the optical absorption spectra are calculated on the corresponding optimized crystal geometries. The generalized gradient approximation (GGA) with the PBE exchange correlation functional was adopted. Test calculations showed that an increase in the number of k-points yields no significantly different results to the total energy (0.1×10^{-2} or so for (b) model) at cutoff energy of 480eV. Optimized structural parameters of *a*, *c* and *u* (*u*=*d*ap/*c*, *d*ap is the apical Ti-O bond length) for pure anatase TiO_2 are listed in Table 1, which showing acceptable consistent with experimental [29] and theoretical predication [30]. A scissors operator of 1.337eV was introduced to shift the conduction levels to consistent with the measured value of the band gap [2, 8, 15].

The absorption curves can be obtained from the imaginary part of the dielectric constant from CASTEP calculation. The imaginary part of the dielectric constant ε_2 is described as:

$$\varepsilon_2(\hbar\omega)=\frac{2e^2\pi}{\Omega\varepsilon_0}\sum_{c,v}\sum_{k}\left|\left\langle\Psi_k^c\left|\hat{u}\cdot r\right|\Psi_k^v\right\rangle\right|^2\delta\left[E_k^c-E_k^v-\hbar\omega\right]$$

Where Ω is the volume of the elementary cell, *k* represents the k point, ω is the frequency of the incident light, *c* and *v* represent the conduction and valence bands, respectively. Ψ_k^c and Ψ_k^v are the eigenstates, **r** is the momentum operator and $\hat{u}$ is the external field vector.

Table 1 Structural parameters of anatase TiO_2.

	This work	Experimental [21]	Theoretical [22]
a (Å)	3.851	3.782	3.692
c (Å)	9.903	9.502	9.671
u	0.205	0.208	0.206

Table 2 Band gap energy of pure and S-doped TiO_2, the value after correction of scissor operator (+1.337eV), the lowering value of band gap corresponding to the band gap of pure TiO_2, Δ, the calculated absorption edge based on the band gap energy, and the distance of the bottom of the impurity state band arising from S doping from the upper edge of valence band, D. The case for anionic S and N doping under the same calculation level are also provided.

	Concentration	Band gap	Scissor operator	Δ (eV)	Absorption edge	D (eV)
pure	0.0000	1.870	3.200		388	
(b)	0.0093	1.454	2.791	0.409	445	0.704
(c)	0.0139	1.218	2.555	0.645	486	0.584
(d)	0.0417	0.704	2.034	1.166	610	0.381
so	0.0417	1.141	2.478	0.729	501	
no	0.0417	1.351	2.688	0.519	462[a]	

a: the data in this "no" row is obtained without spin polarization and provided only for reference.

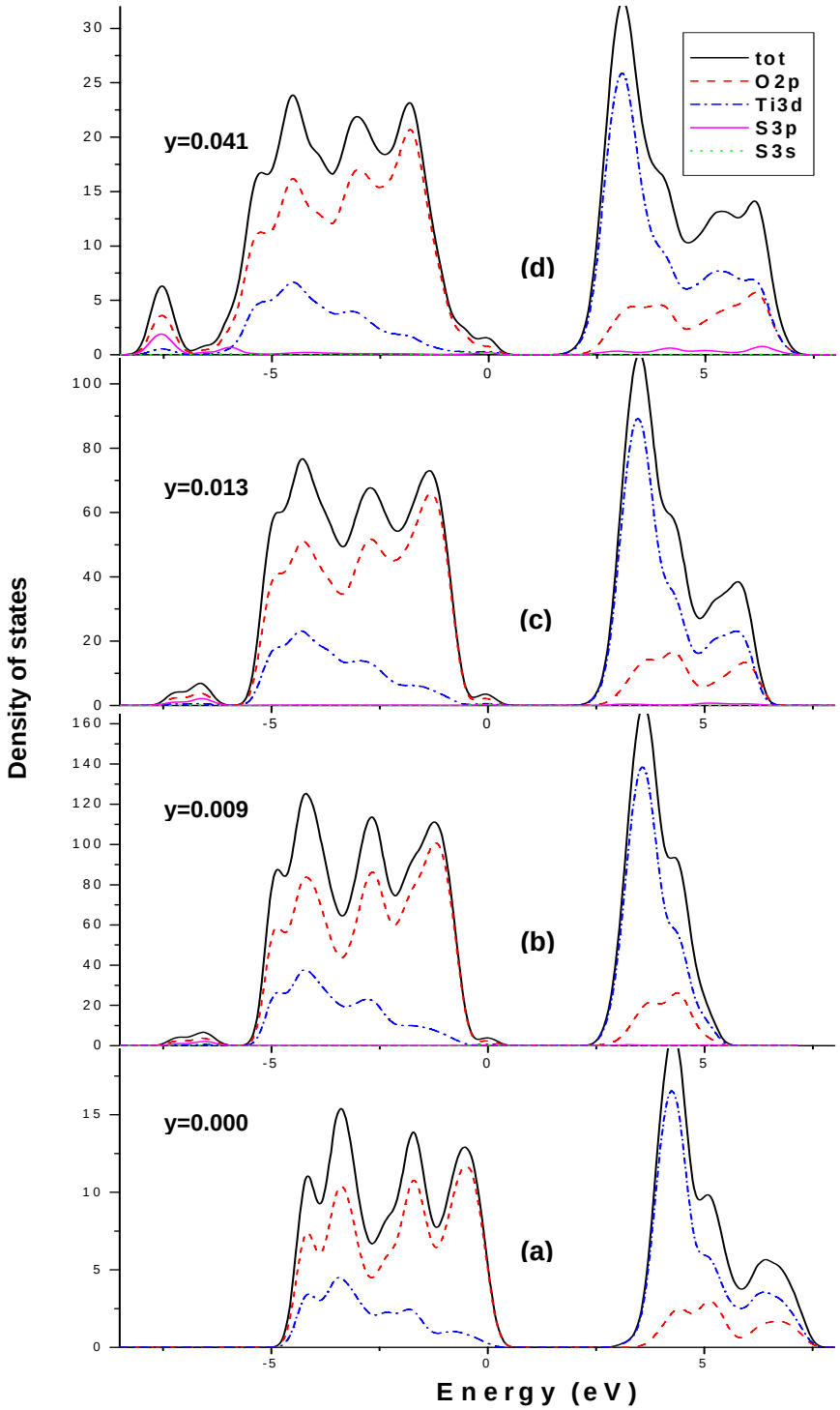

Figure 1 Density of states plots for different levels of S doping in anatase TiO_2. The unit for density of States is states/eV·Unit cell, y: doping concentration.

3. Results and discussions

3.1 *Electronic structure analysis*

Density of states plots calculated for different levels of S doping in the TiO_2 are presented in Figure 1, and indicate how the band gap of the system varies with sulphur content(CASTEP program takes the energy of the highest occupied orbital as the energy zero by default). Figure 2 is a local enlargement of (a) and (d) of Figure 1.

Comparison between pure (a) and doped cases of (b) to (d) indicates clearly that the band gap of TiO_2 is engineered by an impurity state, which is localized slightly above the valence band O2p, just as that in the anionic S doping case [15]. Excitations from the impurity state to conduction band may be responsible for the red shift of absorption edge observed in the cationic S-doped TiO_2 [16-17]. It can be speculated that the presence of the impurity state due to S substituting for Ti induced the visible light activity for $Ti_{1-x}S_xO_2$. This is consistent with a theoretical conclusion of Ohno et al.[17], which also ascribed the origin of the visible light activity of cationic S-doped TiO_2 to the presence of an impurity state on the valence band.

Figure 2 is an enlargement of Figure 1 (a) and (d) designedly to make clear the composition of the impurity state on the upper edge of valence band. It clearly shows that the impurity state is made up of S3p, S3s, Ti3d and O2p, with S3p contributes to both valance and conduction band. On this point, Ohno et al. had a somewhat different view [17]. In their job, they have stated that the impurity state on the upper edge of valence band due to cationic S doping is composed of S3s orbital, while S3p only contributes to conduction band based on electronic structure calculation [17]. From the inorganic chemistry point of view, it is also not so suitable to think of that the outermost valence orbital S3p of S doesn't take part in the bonding. So, we think their understanding is not acceptable. Further analysis on the doping TiO_2 in different doping levels show that the presence of the impurity state and its composition are not changed with the doping concentration, although the percent of each component may be varied (Figure 1).

Moreover, the position of the impurity state reveals that, the alteration of the absorption property of TiO_2 by S substituting for Ti realized still by the interaction between S 3p

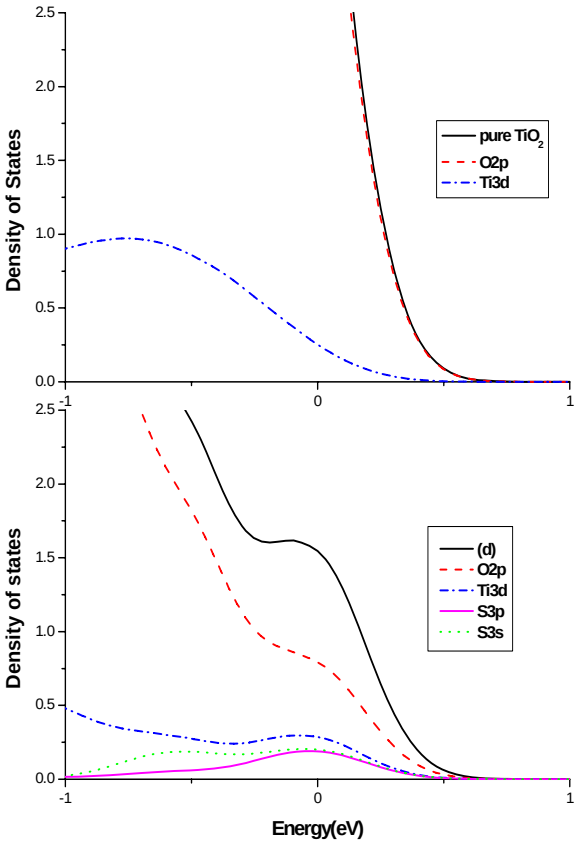

Figure 2 local enlargement of (a) pure and (d) cationic S-doped TiO_2 in Figure 2.

(combining with S3s and Ti3d) and O2p, just like in the anionic S-doped case [13-15]. Its existing type is also similar with that of S3p in the anionic doping cases, being in a slightly localized way above the valence band at low doping concentration, gradually turning into a mixing way along with the doping concentration increasing, as evidenced from the fact of that the distance of the bottom of the impurity state band to the upper edge of valence band reducing with the doping concentration enhancement (Table 2, the last column) [15]. On the other hand, the interaction between S3p and O2p of these two doping cases of S must have some discrepancy intrinsically. Since the local environment of doping S is entirely different. In the cationic S doping, S on the Ti site

interacts with O directly with the formation of six S-O bonds, while the interaction between S and O is indirect in the anionic S doping case where three S-Ti bonds are formed. The interaction strength should be much stronger in the cationic S doping, which is somewhat reflected by the participation of S3s into the valence band.

To make the situation more clearly, we have provided the calculation results for anionic S and N-doped anatase TiO_2 denoted as "so" and "no" with the same calculation level at the doping concentration of 0.0417 (Table 2, the last two rows). Calculation shows there is no separation between impurity state band and valence band for the "so" doping case. Namely, S3p is mixing with O2p in the anionic S doping case when we used a cutoff energy of 480eV (a separation of 0.002eV at 300eV [15]). While a separation of 0.381eV is existing in the cationic S doping case (Table 2). Then the position of the impurity state in the band gap due to cationic doping S is slightly higher above the valence band than that in the anionic S doping case, which can be speculated as the direct reason for the higher absorption of $Ti_{1-x}S_xO_2$, since it shortened the distance of electron transition from the impurity state to the conduction band. This may be an advantage for the absorption and may be disadvantageous for the carrier transfer according to Asahi et al.'s point of view [2]. An extra calculation on a doping level of 0.0833 indicates that the separation in this doping level is reduced to be 0.172 eV, which indicate to us that the mixing between the impurity state and valence band O2p is not far away from this doping level (8.3%). Nevertheless, according to Lin et al, the mixing of N2p and O2p is occurred up to a 20% doping level [8]. So, the position of the impurity state here is not so high. Then, it can be concluded that cationic doped S affects the TiO_2 still in a non-metallic way, with an impurity state functioning on the upper edge of valence band O2p similar to its performance in the anionic doping case.

The concentration-dependent behavior of band gap energy is also evident. Band gap energies of 3.200, 2.791, 2.555 and 2.034eV are corresponding to doping levels of 0.0000, 0.0093, 0.0139, and 0.0417 (Table 2 and Figure 1), respectively. Comparing with the band gap of pure TiO_2, the lowering values by different S doping levels of 0.0000, 0.0093, 0.0139, and 0.0417 are 0.000, 0.409, 0.645 and 1.166eV, respectively (Table 2). An almost linear reduction of band gap energy with the doping concentration enhancement can be found just as disclosed in anionic S, N doping cases [8, 15]. We also find that the width of valence band increases with the doping concentration increasing [15, 31].

In the lattice of TiO_2 crystal, Ti is in a six-coordination. Due to the limitation of rigid regular arrangement of crystal, doping S is very likely to adopt a sp^3d^2 hybridization to satisfy the requirement of six coordination of Ti site. The participation of S3s into the valence band can be evidence to this. While the hybridization must be non-equivalent, since the bond lengths in the doping cases, such as (b), (c) and (d) models, are changed a lot, with two bond lengths equal along x- or y-axis, respectively, while with the bond lengths changed a lot on Z-axis, one is very long and one is very short with a discrepancy up to 0.8Å (Table 3).

Table 3 Population on S atom and bond length of the six S-O bonds in different models.

Model	Population	S-O Bond Length (Å)			
(b)	1.26	1.577	1.874(2)	2.000(2)	2.465
(c)	1.25	1.579	1.882(2)	1.991(2)	2.463
(d)	1.22	1.598	1.904(2)	1.972(2)	2.343

It can conclude that six-coordination makes cationic S more sensitive to the local

environment than the S on a three-coordinated O site. Mulliken population analysis shows that, independent of its concentration in the crystal, the charge on the S ion was about 1.20 (1.26, 1.25, 1.22 for (b), (c) and (d) cases) (Table 3). Similar situation is also found in the anionic S, N-doped cases [8, 15]. The population values for Ti site are +0.88 in the pure TiO_2. It can be deduced that the doping S atom is oxidated largely. The competition of S and Ti beside the center O makes the electron more delocalized in the S-O-Ti linkage.

As a probe of the creditability of calculations, the change trend of the volume of TiO_2 lattice before and after doping was checked in our study. Just as in the anionic S doping [15] that an expansion of the lattice of TiO_2 induced because of the much larger ion radius of S (1.70Å) than O (1.30Å), calculation results shows that the incorporation of the cationic S (0.30Å or so) with a shorter ion radius than Ti (0.74Å) brought a contraction for the unit cell of TiO_2. Calculation results show that the contraction of the unit cell due to cationic S doping is present regardless of doping level and becomes more evident with the doping concentration enhancement. An almost linear relationship between doping level (0.0000, 0.0093, 0.0139 and 0.0417) and volume ratio V/V_0 before and after doping (1.000, 0.998, 0.997, and 0.990) was disclosed (Table 4). Calculations on the anionic S-doped rutile system have also disclosed the same law [31]. It confirmed that our simulation on the cationic S-doped anatase TiO_2 systems is creditable.

Table 4 The relation of V/V_0 ~ doping concentration

Doping level	0.0000	0.0093	0.0139	0.0417
V/V_0	1.000	0.998	0.997	0.990

Note: **V**, the volume of the optimized structure for doped models; $\mathbf{V_0}$, the volume of the optimized structure for the undoped models of the same dimension. $\mathbf{V/V_0}$, the ratio of the optimized volume before and after doping

3.2 Absorption spectra analysis.

Figure 3 indicates the variation of absorption with sulphur content. Red shift of the absorption edge can be found for cationic S doping, regardless of doping concentration. And the red shift is increased with doping level. Calculation indicated that the absorption edge of 388, 445, 486, and 610nm for the pure (a) and (b), (c), and (d) models is corresponding to the doping level of 0.0000, 0.0093, 0.0139, 0.0417. The concentration- dependent absorption behavior disclosed here is consistent very well with the experimental observation of UV-Vis spectra [18].

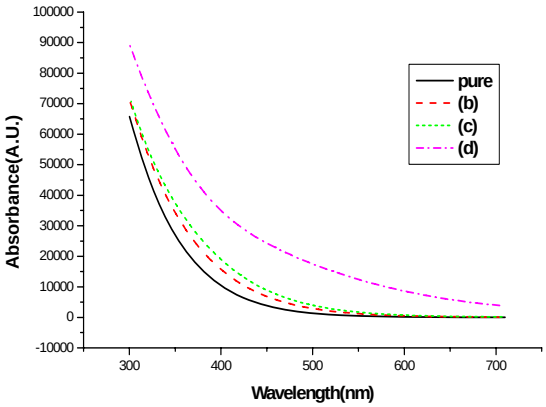

Figure 3 Absorption spectra of cationic S doped TiO_2 with different doping concentration

The different absorption behavior between cationic S- and anionic S, N-doped anatase TiO_2 in the visible light region at one identical doping level (0.0417) was described in Figure 4. As we can see, all the three kinds of doping can extend the absorption edge of TiO_2 to low energy direction. Cationic S-doped TiO_2 (st doping) has the strongest absorption in the visible light region. The next is the anionic S-doped

one, and the anionic N-doped one. Their calculated absorption edge was 610, 501, 462 nm, respectively, as shown in Table 2. A stronger absorption for cationic S-doped TiO_2 comparing to anionic S, N-doped one is confirmed in our DFT study, consisting very well with the experimental investigation [16-17]. Unlike $TiO_{2-x}S_x$, band structure shows that $Ti_{1-x}S_xO_2$ is still an indirect semiconductor. Its higher absorption is achieved by the larger red shift of absorption edge. As for the two anionic doped cases, anionic S-doped TiO_2 has a larger red shift, while N-doped TiO_2 has a shoulder nearly across the whole visible light region, which is in favor of the absorption of materials. So, a comparable absorption for anionic S, N-doped TiO_2 can be expected.

Since the concentration-dependent of absorption behavior in each of the three doping cases is all almost linear, as confirmed in this work and from literatures on the anionic S, N systems [8, 15, 18], we believe this kind of comparison on an identical doping level (0.0417) is accredited.

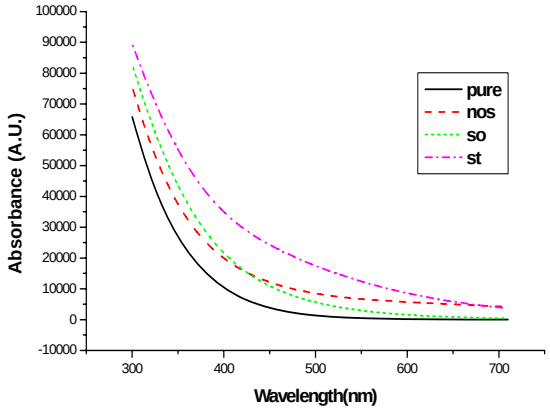

Figure 4 Comparison between no, so, st doping (st, S substituting for Ti; so, S substituting for O; no, N substituting for O) at 0.0417 doping concentration with no doping case obtained by spin-polarized calculation.

4. Conclusion

Electronic structure analysis shows that cationic doped S could induce visible light activity for anatase TiO_2 effectively by providing an impurity state on the upper edge of valence band, in a way similar to the anionic doped S. Concentration dependent behavior of band gap energy and the red shift of absorption edge were evidenced. A stronger absorption for cationic S-doped TiO_2 than anionic S, N-doped one was predicted, because of the higher position of the impurity state in the band gap, which is consistent with experiment results [16-17]. The potential of cationic S-doped TiO_2 for visible light absorption impressed us that it can be a good photocatalyst with visible light activity. Combining the good performance of anionic S-doped TiO_2, it is expected that S-doped TiO_2 may be a potential candidate of photocatalysts more promising than N-doped one.

Acknowledgments

This work was supported by National Natural Science projects (No: 20703027, 20975056 and 20633060), Foundation of Shandong Educational Committee (No: J09LB06), a Strategic Investments Scheme administrated by The Chinese University of Hong Kong, and China Postdoctoral Science Foundation (20080440117) and NSFC (50872158).

References

[1] W. Choi, A. Termin, M. R. Hoffmann, J. Phys. Chem. 98 (1994) 13669-13679.

[2] R. Asahi, T. Morikawa, T. Ohwaki, K. Aoki, Y. Taga, Science 293(2001) 269-271.

[3] H. Irie, Y. Watanabe, K. Hashimoto, J. Phys. Chem. B 107 (2003) 5483-5486.

[4] O. Diwald, T. L. Thompson, E. G. Goralski, S. D. Walck, J. T. Jr. Yates, J. Phys. Chem. B 108 (2004) 52-57.

[5] M. Sathish, B. Viswanathan, R. P. Viswanath, Ch. S. Gopinath, Chem. Mater. 17 (2005) 6349-6353.

[6] R. Nakamura, T. Tanaka, Y. Nakato, J. Phys. Chem. B 108 (2004) 10617-10620.

[7] C. Di Valentin, G. Pacchioni, A. Selloni, S. Livraghi, E. Giamello, J. Phys. Chem. B 109 (2005) 11414-11419.

[8] Zh. Lin, A. Orlov, R. M. Lambert, M. C. Payne, J. Phys. Chem. B 109 (2005) 20948-20952.

[9] S. U. M. Khan, M. Al-Shahry, W. B. Ingler, Jr. Science 297 (2002) 2243-2245.

[10] W. Zhao, W. Ma, Ch. Chen, J. Zhao, Zh. Shuai, J. Am. Chem. Soc. 126 (2004) 4782-4783.

[11] L. Lin, W. Lin, Y. Zhu, B. Zhao, Y. Xie, Chem. Lett. 34 (2005) 284-285.

[12] D. Li, H. Haneda, Sh. Hishita, N. Ohashi, Chem. Mater. 17 (2005) 2596-2602.

[13] T. Umebayashi, T. Yamaki, H. Itoh, K. Asai, Appl. Phys. Lett. 81 (2002) 454-456.

[14] T.Umebayashi, T. Yamaki, S. Tanaka, K. Asai, Chem. Lett. 32 (2003) 330-331.

[15] F. H. Tian, Ch. B. Liu, J. Phys. Chem. B 110 (2006) 17866-17871.

[16] T.Ohno, T. Mitsui, M. Matsumura Chem. Lett. 32 (2003) 364-365.

[17] T. Ohno, M. Akiyoshi, T. Umebayashi, K. Asai, T. Mitsui, M. Matsumura, Appl. Catal. A-Gen. 265 (2004) 115-121.

[18] J. C. Yu, W. Ho, J. G. Yu, H. Yip, P. K. Wong, J. C. Zhao, Environ. Sci. Technol. 39 (2005) 1175-1179.

[19] H. Kisch, W. Macyk, ChemPhysChem 3 (2002) 399-400.

[20] H. Li, X. Zhang, Y. Huo, J. Zhu, Environ. Sci. Technol. 41 (2007) 4410-4414.

[21] F. H. Tian, C. Liu, D. Zhang, A. Fu, Y. Duan, S. Yuan, Jimmy C. Yu, ChemPhysChem 11 (2010) 3269-3272.

[22] R. Long and N. J. English, J. Phys. Chem. C 113 (2009) 8373-8377.

[23] S. S. Soni, M. J. Henderson, Jean-Francois Bardeau, A. Gibaud, Adv. Mater. 20 (2008) 1493-1498.

[24] P. Periyat, S. C. Pillai, D. E. McCormack, J. Colreavy, S. J. Hinder, J. Phys. Chem. C 112 (2008) 7644-7652.

[25] J. Wang, D. N. Tafen, J. P. Lewis, Z. Hong, A. Manivannan, M. Zhi, M. Li, N. Wu, J. Am. Chem. Soc. 131 (2009) 12290-12297.

[26] J. A. Rengifo-Herrera, K. Pierzchała, A. Sienkiewicz, L. Forro´, J. Kiwi, J. E. Moser, C. Pulgarin, J. Phys. Chem. C 114 (2010) 2717-2723.

[27] S. A. Shevlin and S. M. Woodley, J. Phys. Chem. C 114 (2010) 17333-17343.

[28] M. D. Segall, P. L. D. Lindan, M.J. Probert, C. J. Pickard, P. J. Hasnip, S. J. Clark, M.C. Payne, J. Phys.: Condens. Matter 14 (2002) 2717-2744.

[29] J. K.Burdett, T. Hughbandks, G. J. Miller, J. W. Richardson, J. V. Smith, J. Am. Chem. Soc. 109 (1987) 3639-3646.

[30] R. Asahi, Y. Taga, W. Mannstadt, A. J. Freeman, Phys. Rev. B 61 (2000) 7459-7465.

[31] T. Yamamoto, F. Yamashita, I. Tanaka, E. Matsubara, A. Muramatsu, Mater. Trans. 45 (2004) 1987-1990.